Journal of Chromatography A 1616 (2020) 460774

Contents lists available at ScienceDirect

Journal of Chromatography A

journal homepage: www.elsevier.com/locate/chroma

Effect-directed profiling and identification of bioactive metabolites from field, *in vitro*-grown and acclimatized *Musa* spp. accessions using high-performance thin-layer chromatography-mass spectrometry

Ibukun O. Ayoola-Oresanya[a,b,c], Mubo A. Sonibare[a], Badara Gueye[b], Rajneesh Paliwal[b], Michael T. Abberton[b], Gertrud E. Morlock[c,*]

[a] Department of Pharmacognosy, Faculty of Pharmacy, University of Ibadan, Ibadan, Nigeria
[b] Genetic Resources Centre, International Institute of Tropical Agriculture, Ibadan, Nigeria
[c] Department of Food Science, Institute of Nutritional Science, Justus Liebig University Giessen, Giessen, Germany

ARTICLE INFO

Article history:
Received 19 October 2019
Revised 5 December 2019
Accepted 6 December 2019
Available online 9 December 2019

Keywords:
Musa spp.
Antioxidants
Effect-directed analysis
In vitro culture
Genetic fidelity
HPTLC-HRMS

ABSTRACT

Bananas and plantains (*Musa* spp.) are used as nutritious foods, and at the same time, are a source of phytoconstituents for the pharmaceutical industry. As biological activities of especially the pulp and peel of *Musa* spp. have been documented, this study investigated the variation in the secondary metabolite profiles of the leaves from field, *in vitro*-grown and acclimatized accessions. The genetic fidelity of the diverse accessions was assessed using diversity array technology sequencing. It showed that the *in vitro*-grown accessions were true-to-type with the field samples. The antioxidant and anticholinesterase activities of the samples from different culture systems (field and *in vitro*) were evaluated by UV-spectrophotometry and compared to high-performance thin-layer chromatography-effect-directed analysis (HPTLC-EDA). The latter was applied for the first time for effect-directed profiling of the polar and medium polar sample components via different biochemical and biological assays. Compound zones showed acetyl-/butylrylcholinesterase inhibition (zones 1–4), α-/β-glucosidase inhibition (zones 1 and 2) as well as antioxidative (zones 1–3) and antimicrobial (zone 4) activities. Structures were preliminary assigned by HPTLC-HRMS. The HPTLC was effective for bioactivity-guided characterization of the bioactive constituents in *Musa* spp. accessions. Accumulation of useful metabolites, especially compounds with antioxidant and anticholinesterase properties, was higher in samples from *in vitro* system. This validated the use of plant tissue culturing as an alternative method for large scale production of plant material and supply of bioactive constituents.

1. Introduction

High-performance thin-layer chromatography (HPTLC) is a robust, simple, rapid, and efficient tool in the quantitative analysis of compounds. It enables a highly sensitive high-throughput screening for the rapid analysis of a large number of compounds [1]. It is widely used for quality control of medicinal plants and characterization of metabolites. Bioassays with cuvette, petri dish and microtiter plates gives a sum of parameters, which can be due to antagonistic or synergistic effects but the specific compounds responsible for the bioactivity are unknown. Biological and biochemical assays can be combined with chromatography and reveal the bioactivity of single compounds. The effect-directed analysis (EDA), in combination with chromatography, makes detection and characterization of bioactive compounds in plant samples easier. Thus, thousands of compounds in a complex plant mixture are reduced to few important bioactive ones [2]. Several researchers have developed HPTLC-enzyme inhibition assays and other bioassays, *e.g.*, cholinesterase and glucosidase inhibition [3,4]. In the past, to get structural information about unknown compounds, HPLC was in most cases combined with high-resolution mass spectrometry (HRMS) [5], while the hyphenation of HPTLC with spectrometric/spectroscopic detectors received little attention in analytical chemistry [6]. The isolation and online transfer of zones of interest to a mass spectrometer became easier with the availability of the first TLC–MS interface introduced in 2009 [7]. More so, it was possible with MS^2 experiments to assign molecule ions and their fragment ions. This powerful hyphenation of HPTLC to HRMS ensured a fast, quantitative, reproducible, high-throughput, precise

* Corresponding author.
E-mail address: Gertrud.Morlock@uni-giessen.de (G.E. Morlock).

https://doi.org/10.1016/j.chroma.2019.460774
0021-9673/

and cheap analysis [8]. However, the complete structure elucidation of a molecule requires in addition nuclear magnetic resonance (NMR) analysis [9], especially in the case of a new and novel compound. These techniques are important, especially in the recent search for bioactive molecules in *Musa* spp.

Musa spp. (bananas and plantains), belonging to the family Musaceae, are not only important food crops but have also been reported for various medicinal uses. Traditionally, dried fruits of banana, the flowers and roots are used orally for diabetes [10]; the extracts from the leaves are used for wound healing [11] and fruit as a mild laxative [12]. Other pharmacological activities, reported for different parts of *Musa* spp., include anti-ulcer, hypoglycemic and antimicrobial activities among others [13,14]. It is therefore an important species for the production of bioactive secondary metabolites. Plant tissue culture is an alternative method of plant material supply for the production of desirable medicinal compounds from *Musa* spp. leaves. It is a less destructive source of plant material compared to field and also ensures sustainable conservation and rational utilization of biodiversity [15]. *In vitro* plant tissue culture tool can be a reliable supplemental method to traditional agriculture in the industrial production of bioactive plant metabolites [16]. However, true-to-type clonal fidelity is one of the most important pre-requisites in the micropropagation of plant species. The occurrence of cryptic genetic defects potentially arising via somaclonal variation in plants regenerated *in vitro* can limit the broader utility of the micropropagation system [17]. Therefore, it is necessary to establish genetic uniformity of micropropagated plants to confirm the quality of the plantlets for its commercial utility.

In the past, other chromatographic methods have been used for the detection of phytochemicals in *Musa* spp. Thin-layer chromatography (TLC) analysis was used to confirm the presence of flavanoids in the *Musa* spp. extract [18]. Anthocyanins and their derivatives have also been identified from different parts of *Musa.* The volatile fractions of the pulp and whole fruit of two banana cultivars were characterized by [19] using headspace solid phase micro-extraction (HS-SPME) and gas chromatography–mass spectrometry (GC–MS). Vilela et al. [20] also identified fatty acids and sterols in the pulp of different banana cultivars using GC–MS. Sonibare et al. [21] characterized field-grown *Musa acuminata* leaves using ultra performance liquid chromatograpghy quadrupole time of flight (UPLC-QToF)-MS. This analysis revealed the presence of flavonoids, fatty acids and sugars. Phytoanticipin, a strong antifungal agent, was isolated in *Musa* spp. using bioassay-guided vacuum liquid chromatography (VLC) purification and LC-MS for characterization [22]. Several researchers have also reported various biological activities of *Musa* spp. using majorly cuvette assays, spectrophotometric methods and *in vivo* animal models [13,14,23]. Report on HPTLC analysis of *Musa* in literature is scarce; Bonnet et al. [24] reported the use of an HPTLC method for the quantification of dopamine in the peel of the Cavendish banana.

HPTLC-EDA-HRMS has not been exploited for a straightforward characterization of bioactive secondary metabolites in *Musa* spp. so far. Thus in this study, HPTLC was hyphenated to acetyl and butyryl cholinesterase, α-glucosidase, β-glucosidase, α-amylase, *Aliivibrio fischeri, Bacillus subtilis* and *Salmonella thyphimurium* assays, which was aimed at identifying bioactive molecules with multiple biological activities in *Musa* spp. The suitability of HPTLC for a high throughput bioprofiling was evaluated on 15 different taxonomic reference *Musa* spp. accessions comprising different genome groups of *Musa acuminata* and *Musa balbisiana,* which are representatives of *Musa* spp. global biodiversity. This was combined with a comparative study of the bioactivity of field, *in vitro*-grown and acclimatized taxonomic reference accessions reported for the first time.

2. Material and methods

2.1. Reagents and chemicals

All chemicals used in the study were of analytical grade. They include gallic acid, anhydrous sodium carbonate, sodium acetate, aluminum chloride, sodium hydroxide, Fast Blue B salt, acetic acid, citric acid, α-naphthyl acetate, acetylcholinesterase (AChE) lyophylisate (Electrophorus electricus, electric eel), butyrylcholinesterase (BChE) from horse serum, hydrochloric acid (32%), α-glucosidase from *Saccharomyces cerevisiae* (1000 U/vial), α-amylase from hog pancreas (50 U/mg), sodium chloride, sodium monohydrogen phosphate, bovine serum albumin (BSA), tris(hydroxymethyl)aminomethane (TRIS), eserine, Folin–Ciocalteu reagent, quercetin, acetylthiocholine iodide (ATCI), 5,5′-dithiobis [2-nitrobenzoic acid] (DTNB), 2,2-diphenyl-1-picrylhydrazyl (DPPH$^{\bullet}$), 2,4,6-Tri(2-pyridyl)-s-triazine (TPTZ), ferric chloride hexahydrate, ascorbic acid, 6–hydroxy–2,5,7,8-tetramethylchroman-2-carboxylic acid (trolox), physostigmine, acarbose, imidazole, 2-naphtyl-α-D-glucopyranoside, 2–chloro–*p*-nitrophenyl-α-D-maltotrioside (CNP-G3) and formic acid, were obtained from Sigma-Aldrich (Steinheim, Germany). 2-Naphthyl-β-D-glucopyranoside (95%) and β-glucosidase from almonds (3040 U/mg) were provided by ABCR, Karlsruhe, Germany. 1-Naphthyl acetate was obtained from AppliChem, Darmstadt, Germany. 3-(4,5-Dimethylthiazol-2-yl)−2,5-diphenyltetrazoliumbromide (MTT, ≥98%), methanol, ethanol (95%), ethyl acetate, *Bacillus subtilis* spores (BGA, ATCC 6633), and toluene as well as HPTLC plates silica gel 60 F_{254}, 20 × 10 cm, were purchased from Merck, Darmstadt, Germany. Luminescent marine bacteria *Aliivibrio fischeri* (DSM no. 5171) were obtained from the Leibniz Institute, DSMZ, German Collection of Microorganisms and Cell Cultures (Braunschweig, Germany). Natural products reagent (NP, diphenylboryloxyethylamine or diphenylboric acid β-ethylamino ester) were purchased from Carl Roth, Karlsruhe, Germany.

2.2. Plant materials

Accessions from the *Musa* taxonomic reference collection (15) were collected from the Genetic Resource Centre, International Institute of Tropical Agriculture (IITA), Ibadan, Nigeria. These accessions were selected based on their genome group. They comprise *Musa acuminata* and *Musa balbisiana* species, which are representatives of *Musa* biodiversity. More accessions, landraces (10) from IITA and a *Musa sapientum* accession from the Botanical Garden of the University of Ibadan were also selected for the genetic fidelity study. The passport data of the *Musa* spp. used is given in Table S-1.

2.3. In vitro *propagation and acclimatization*

All the *in vitro* materials used were obtained through meristem regeneration from suckers of the accessions, collected from the field and established *in vitro* culture using the IITA *in vitro* genebank routine protocol [25]. The sterilization and *in vitro* propagation protocol used is as described by Ayoola et al. [26], using Murashige and Skoog basal medium supplemented with growth hormones (0.18 mg/L of indole-acetic acid and 4.5 mg/L of benzyl amino purine) [27]. Plantlets with a well-developed root were carefully washed free of agar, transferred to a prepared pot containing sterile top soil and covered with a wet plastic bag for humidity. Pots were maintained in an insect-proof room with a warm and bright environment. The plastic bags were removed after 10 weeks and plantlets were left to grow for up to 7 months.

2.4. DNA extraction and diversity array technology sequencing (DArTseq) single-nucleotide polymorphism (SNP) analysis

Genomic DNA was obtained from each field (26) and *in vitro*-grown (26) accessions using 150 mg of young leaves from both field and *in vitro* samples according to CTAB protocol [28] with some modifications [29]. The quality and quantity of all the extracted DNA samples were checked on Nanodrop spectrophotometer and further confirmed on 1% agarose gel run in TAE buffer at 100 V. A total of 56 high quality DNA samples (50 μL of 100 ng μL^{-1}) including four technical replicates as control for sequencing error from three accessions Orishele (field), Simili radjah (both field and *in vitro*) and Safet velchi (*in vitro)* (Table S-1) were sent to Diversity Array Technology (http://www.diversityarrays.com), Canberra, Australia to generate SNP markers. SNP markers was generated using next generation high-throughput DArTseq approach which represents a combination of both complexity reduction using restriction enzymes method [30]. Sequence generated in FASTQ files were further processed using proprietary DArT analytical pipelines. The discovered SNP were run against the phytozome database '*Musa acuminata* DH Pahang v2' which was used as the reference genome. A total of 150556 SNP was derived from DArTseq approach and further filtered based only on minor allele frequency (MAF) >0.01 as there was no missing data after imputation. Data filter, MAF, heterozygosity analysis, pairwise identity-by-state (IBS) genetic distance matrix and genetic relationship cladogram analysis-based IBS matrix using neighbor-joining (NJ) method were completed using Tassel 5.2.25 software [31]. Heterozygosity results were taken into Excel to generate MAF and heterozygosity distribution plot. Similarly, IBS genetic distance matrix was used in R-program [32] with ggplot and gplots packages.

2.5. Preparation of plant extracts

Young leaves from the field (the first and second leaves), 6 weeks old *in vitro*-grown leaves and 7 months old acclimatized leaves were collected, freeze dried and separately milled into powder. Powdered field samples (50 g), 3 g *in vitro*-grown and 5 g acclimatized samples were weighed. They were extracted in methanol (plant sample-to-methanol 1:10, w/v). Extracts were filtered and concentrated *in vacuo*. These residues were stored at 4 °C and 2.5 mg each were re-dissolved in 1 mL methanol for HPTLC analysis.

2.6. UV spectrophotometry for evaluation of antioxidative activity

2.6.1. Total phenolic content (TPC) and total flavonoid content (TFC)

The method of Khatoon et al. [33] was used to evaluate the total phenolic content (TPC) of all the extracts. Blue colored complex are formed when samples containing phenolic compounds were reduced by the Folin–Ciocalteu reagent. Total phenolic content was expressed as mg gallic acid equivalent (GAE)/g extract which was calculated from the regression equation of gallic acid calibration curve ($y = 0.0095x + 0.1325$, $r^2 = 0.9793$). Aluminum chloride colorimetric method was used to evaluate the total flavonoid contents of the plant samples [34]. The TFC was expressed as mg quercetin equivalent (QE)/g extract, calculated from standard curves ($y = 0.0077x + 0.0884$, $r^2 = 0.9980$) prepared with 6.25–200 μg quercetin/mL.

2.6.2. ***DPPH• cuvette assay***

The antioxidant potential of the extracts was determined by their ability to scavenge the stable radical DPPH• according to the method described by Susanti et al. [35] and Ayoola et al. [26] with slight modifications. Briefly, 3 mL of freshly prepared DPPH• solution (0.1 mM) in methanol was mixed with 2 mL of the extract/standard at different concentrations (1.6 to 100.0 μg/mL). Absorbance was measured at 517 nm using a UV/visible spectrophotometer after incubation at room temperature for 30 min in the dark. The experiment was carried out in triplicate. The percentage inhibition of DPPH• free radical scavenging activity was calculated using the following equation:

$$\%\,\text{inhibition} = [(\text{absorbance of control} - \text{absorbance of test sample}/\text{absorbance of control})] \times 100\%.$$

The antioxidant activity of each sample was expressed in terms of IC_{50} (micromolar concentration required to inhibit DPPH• radical formation by 50%), which was calculated from the linear regression curve.

2.6.3. Ferric reducing antioxidant power (FRAP) cuvette assay

The determination of antioxidant activity through FRAP was carried out according to literature [21,36]. The FRAP reagent was freshly prepared using 300 mM acetate buffer, pH 3.6 (3.1 g sodium acetate trihydrate, plus 16 mL glacial acid made up to 1:1 with distilled water). TPTZ (10 mM) in 40 mM hydrochloric acid and 20 mM ferric chloride hexahydrate in the ratio of 10:1:1 was used as the working reagent. The FRAP reagent (2.85 mL) was added to 200 μL extracts and the absorbances were taken at 595 nm wavelength with a spectrophotometer after 30 min. The calibration curve of trolox was used to estimate the activity capacity expressed as mg trolox equivalents per g extract (mg TE/g extract).

2.6.4. Anticholinesterase cuvette assay

The inhibition of acetylcholinesterase was determined spectrophotometrically using the modified Ellman's colorimetric method [37,38]. Samples, eserine, DTNB and substrate (acetylcholine iodide, ATCI) were dissolved in phosphate buffer (pH 8.0). In a 96-well plate, the reaction mixture consisted of 40 µL phosphate buffer (pH 8.0), 20 µL of varying concentrations of the test samples (0.1 to 1 mg/mL of sample and 0.06 to 0.5 mg/mL of positive control, eserine) and 20 µL of the enzyme (0.26 U/mL). The reaction mixture was incubated for 30 min at 37 °C, and then 100 µL of 3 mM DTNB was added. The reaction was initiated by the addition of 20 µL of 15 mM ATCI. The rate of hydrolysis of ATCI was then determined spectrophotometrically by measuring the change in the absorbance per minute (ΔA/min) due to the formation of the yellow 5-thio-2-nitrobenzoate anion at 405 nm over a period of 4 min at 30 s interval. Buffer was mixed with the enzyme alongside other reagents and served as negative control. The experiments were carried out in triplicate and percentage inhibition was calculated as follows: $\Delta A = (1 - a/b) \times 100$, where a is ΔA/min of test sample and b is ΔA/min of negative control. IC_{50} was calculated from the linear regression curve by plotting the percentage inhibition against extract concentration.

2.7. Statistical analysis

Each antioxidant activity assay was done three times from the same extract in order to determine their reproducibility. Analysis of variance was used to test any difference in antioxidant activities resulting from these methods. Duncan's new multiple range test was used to determine significant differences. Correlations among data obtained were calculated using Pearson's correlation coefficient (r).

2.8. HPTLC-EDA method

2.8.1. Separation system

Apart from the cholinesterase assay (15 or 25 µL/band), 10 µL/band were sprayed on the HPTLC plate for all other assays by an automatic TLC sampler (ATS 4, CAMAG, Muttenz, Switzerland)

using 7-mm bands, 8-mm distance from the lower edge and automatic track distance. After mobile phase development, a polar, acidic solvent system (ethyl acetate - toluene - formic acid - water, 3.4: 0.5: 0.7: 0.5) as well as a medium polar solvent system (toluene - ethyl acetate – methanol, 6: 3: 1) were used to separate most of the plant components. The development was done in an unsaturated 20 cm × 10 cm Twin Trough Chamber (CAMAG) up to a migration distance of 60 mm, which took *ca.* 30 min. The chromatogram was documented by the TLC Visualizer Documentation System (CAMAG) UV lamp at UV 254 nm and 366 nm (CAMAG).

2.8.2. Post-chromatographic derivatization

The chromatogram developed in the polar, acidic mobile phase was derivatized using a reagent sequence. After intermediate drying, the same plate was dipped (1) first in NP reagent, (2) followed by ninhydrin reagent and (3) lastly diphenylamine aniline (DPA) reagent. The plates were heated on the TLC Plate Heater (CAMAG) at 110 °C for 3 to 5 min before dipping in NP reagent, and thereafter documented at UV 366 nm. After immersion in either ninhydrin or DPA reagents, the plates were heated at 110 °C for 3 to 5 min and documented at white light illumination. The chromatograms developed in the medium polar mobile phase were immersed in *p*-anisaldehyde sulfuric acid reagent and heated at 110 °C for 3 to 5 min. For all, immersion time was 2 s at a 2.0-cm/s immersion speed using the TLC Immersion Device, CAMAG.

2.8.3. Neutralization of chromatograms

After development in the acidic mobile phase, chromatograms were neutralized using the Derivatizer (CAMAG) according to Elufioye et al. [38]. Briefly, before the assay application, the chromatograms were dried in a stream of cold air, and phosphate buffer (8%, pH 7.5) was piezoelectrically sprayed on the plates, followed by plate drying in the Automatic Development Chamber (ADC 2, CAMAG).

2.8.4. ***HPTLC-DPPH$^{\bullet}$ assay***

The chromatogram was immersed (immersion speed 2.0 cm/s and immersion time 5 s) in 0.02% methanolic DPPH$^{\bullet}$ solution. The chromatogram was documented at white light illumination (reflection and transmission mode) after 1, 10 and 30 min. The absorbance of the chromatogram was measured at 546 nm using the mercury lamp in the fluorescence mode without optical filter.

2.8.5. HPTLC-AChE/BChE inhibition assays

The cholinesterase inhibition profiling was performed according to Azadniya et al. [39]. The sample volume sprayed as 7-mm bands was 25 µL/band for the polar, acidic mobile phase, but 15 µL/band for the medium polar mobile phase, while the other HPTLC conditions remained the same as described. The positive control was a methanolic physostigmine solution (0.1 to 1 ng/band). Briefly, the neutralized chromatogram was piezoelectrically sprayed with 1 mL TRIS buffer 0.05 M, pH 7.8, then with 3 mL enzyme solution (6.66 AChE units/mL or 3.34 BChE units/mL in 100 mL TRIS buffer, 0.05 M, pH 7.8, containing 1 mg/mL BSA). The plate was incubated at 37 °C for 25 min and piezoelectrically sprayed with the substrate solution (90 mg α-naphthyl acetate and 160 mg Fast Blue B salt in 90 mL water - ethanol, 2:1), followed by drying at room temperature. White inhibition zones were detected on a purple background at white light illumination (transmission and reflection modes).

2.8.6. HPTLC-α-glucosidase, -β-glucosidase and -α-amylase inhibition assays

The glucosidase inhibition profiling were performed according to Jamshidi Aijdi et al. [40]. As ethanolic positive control solutions, acarbose (3 to 18 µg/band) or imidazole (3 to 7 µg/band) were used. Concisely, 2 mL substrate solution (60 mg 2-naphtyl-α-D-glucopyranoside or respective β-anomer in 50 mL ethanol) were piezoelectrically sprayed on the neutralized chromatogram and air-dried for 2 min. The plate was pre-wetted with 1 mL sodium acetate buffer (pH 7.5). Then, 2 mL enzyme solution (100 units α-glucosidase or 200 units β-glucosidase in 10 mL buffer) were sprayed. The plate was placed horizontally in a pre-prepared humidity box and incubated at 37 °C for 15 min for α-glucosidase or 30 min for β-glucosidase. Finally, 0.5 mL of an aqueous Fast Blue B salt solution (2 mg/mL) was sprayed on the chromatogram. Plate images were taken directly and after plate drying (via the ADC 2 humidity control) at white light illumination (transmission and reflection modes). Enzyme inhibitors were detected as white zones on a purple background. For the HPTLC-α-amylase inhibition assay, plates were dipped into the ethanolic substrate solution (1.4 mg/mL CNP-G3), dried for 2 min (hair dryer) and immersed in the enzyme solution (1.2 mg/mL α-amylase in sodium acetate buffer, pH 7.5). After 15 min incubation at 37 °C in a moistened polypropylene box, the autogram was dried and documented at white light illumination. Active compounds were detectable as bright zones against a yellowish green background [41].

2.8.7. HPTLC-Bacillus subtilis *bioassay*

The Gram-positive antibacterial profiling was performed according to Jamshidi-Aidji and Morlock [42]. The positive control was a methanolic tetracycline solution (0.4 to 1.2 ng/band). Briefly, the chromatogram developed in the medium polar mobile phase was dipped for 7 s at an immersion speed of 3 cm/s into the *B. subtilis* suspension (optical density at 600 nm of 0.8), incubated at 37 °C for 2 h and then visualized by immersion into a 0.2% PBS-buffered MTT solution for 1 s at an immersion speed of 3.5 cm/s and incubated at 37 °C for 30 min, followed by heating at 50 °C for 10 min. Active microorganisms reduced the MTT into the purple formazan. Thus, white antimicrobial zones were observed on a purple background [43] and documented at white light illumination (reflection mode).

2.8.8. HPTLC-Aliivibrio fischeri *bioassay*

The Gram-negative antimicrobial profiling was performed according to Krüger et al. [44]. The positive control (PC) was a methanolic caffeine solution (0.5 to 6 µg/band). Briefly, the chromatogram developed in the medium polar mobile phase was immersed for 2 s into the luminescent *A. fischeri* suspension prepared according to European Committee for Standardization [45] (the proper luminescence was visually checked by shaking the flask in a dark room). The change over time of the instantly luminescent bioautogram was monitored for 30 min and documented with the BioLuminizer (CAMAG) using an exposure time of 30 s and 1 min trigger intervals. Dark zones indicated the luminescence inhibition of the bacteria and thus a lower bacterial metabolic activity [46].

2.8.9. HPTLC-SOS-Umu-C bioassay

A genotoxic assay with *Salmonella thyphimurium* bacteria (SOS-Umu-C bioassay), newly developed in a parallel research study [47], was applied on the samples to indicate any genotoxic substances or mutagens in the samples. The standard 4-nitroquinoline-1-oxide was used as a positive control.

2.9. HPTLC-ESI-HRMS

The HPTLC plates were pre-washed by development (up to 9.5 cm each) twice with methanol–formic acid 10:1 (*V*/*V*), followed with acetonitrile–methanol 2:1 (*V*/*V*) [48]. The *Musa* spp. leaf extracts were applied in triplicate (as three sets) and developed. The chromatogram was cut (smartCut Plate Cutter, CAMAG). The first

section was used for the bioassay, the second section for derivatization (with either natural product reagent for the polar, acidic mobile phase or anisaldehyde sulfuric acid reagent for the medium polar mobile phase), while the third section was for HRMS recording. For the latter, the positions of the active zones were transferred on the chromatogram for HRMS and marked at UV 254 or 366 nm using a soft pencil. The zones were eluted with methanol (flow rate 0.1 mL/min) using the TLC-MS Interface 2 (CAMAG) or Plate Express (Advion, Ithaca, NY) coupled to the QExactive Plus mass spectrometer (Thermo Fisher Scientific, Dreieich, Germany). Full scan mass spectra (*m/z* 50−800) were recorded in the positive and negative ionization modes with the following settings: ESI voltage 3.3 kV, capillary temperature 320 °C, and collision energy 35 eV. Nitrogen was produced by a SF2 compressor (Atlas Copco Kompressoren and Drucklufttechnik, Essen, Germany). Data evaluation and background subtraction were performed by Xcalibur 3.0.63 software (Thermo Fisher Scientific).

3. Results and discussion

3.1. In vitro *propagation and genetic conformity between field- and* in vitro-*grown* Musa *spp. accessions*

The results of this study confirmed that biomass production from *Musa* spp. is possible within a short time using *in vitro* propagation (Fig. S-1). This method is not restrained by environmental conditions and can also give good extraction yield, like field material. This method confirms the amenability of *Musa* spp. to plant tissue culture reported by several studies [49–51].

From the DArTseq analysis, a total of 150.5 K SNP markers were generated with imputation for missing markers and further filtered for MAF >0.01 and retained 114285 SNPs which was used for the genetic fidelity study. Out of 114 K SNP, 93524 SNP were distributed all over 11 chromosomes of banana genome (Table S-2) and 20064 SNPs were not aligned on reference genome, while 697 SNPs were distributed on 12 chromosomes of mitochondrial genome. Minor allele frequency ranged from 0.018 to 0.50 (Fig. S-2). The proportion of heterozygous ranged from 0.009 to 0.2436 (Fig. S-3) in both field and *in vitro* samples and the average heterozygosity proportion was 0.12. The pairwise genetic distance matrix among the *Musa* spp. accessions ranged from 0.0199 to 0.4968 between the 56 field- and *in vitro*-grown samples (Fig. S-4). The pairwise IBS genetic distance found 23 out of the 26 accessions true to type between *in vitro* and field material except Egjoga, P. raja and P. Jaribuaya accessions and seen in the Neighbor Joining (NJ) clustering based on IBS genetic distance matrix (Fig. 1). The genetic distance based on NJ-tree mapping showed that the true-to-type field and *in vitro*-grown accessions were grouped together based on their genetic similarity. Similar result was obtained from the heterozygosity proportion distribution of the 56 banana samples. Molecular markers (*e.g.*, SSR, ISSR and RAPD) have been widely used in crops for genetic relationship analysis [52–54] including SNP markers [55–56] that are most widely accepted nowadays in worldwide molecular research. This study suggests that banana accessions, which are true-to-type between field and *in vitro* lines, can be used for large biomass production of *Musa* spp. within a short time using *in vitro* plant tissue culture and supply of secondary metabolites.

3.2. Total phenolic (TPC) and flavonoid (TFC) content

The total phenolic and total flavonoid content varied considerably among the accessions. Many of the accessions have high phenolic content. The total phenolic content ranged from 2.4 ± 0.3 to 124.5 ± 12.7 mg GAE/g extract with both field and *in vitro*-grown simili radjah (ABB) having the highest phenolic content, while the total flavonoid content ranged from 0.4 ± 0.1 to 60.1 ± 6.3 mg QE/g extract (Table 1). Field and *in vitro*-grown *Musa balbisiana* Tani (BBwild), *Musa balbisiana* HND (BBwild) and Dole (ABB) had consistently low total phenolic and total flavonoid contents. Across all the tested accessions, *in vitro*-grown samples had higher total phenolic content whereas, field-grown leaf samples had higher total flavonoid content.

3.3. Total antioxidative and anticholinesterase activity

All the samples showed a dose dependent DPPH$^{\bullet}$ free radical scavenging activity by reducing the purple colored and stable DPPH$^{\bullet}$ radical to the yellow-colored diphenylpicrylhydrazine**.** The values of the concentration of the extract that can give 50% inhibition (IC_{50}) ranged from 10.7 ± 0.3 to 257.9 ± 2.3 µg/mL (Table 1). *In* vitro-grown samples gave the highest antioxidant activity when compared to their field counterpart. Similar result was obtained from previous study [25]. FRAP assays are widely used to determine the efficiency of antioxidant compounds in plants to compete with the FRAP reagent and reduce the ferric to the ferrous blue-colored TPTZ complex. The trolox equivalent ranged from 4.3 ± 0.1 to 152.2 ± 2.8 mg TE/g extract with *in vitro*-grown samples again having better antioxidant activity. *Musa balbisiana* Tani (BBwild) and *Musa balbisiana* HND (BBwild) exhibited low antioxidant potential in these assays. For the AChE inhibition, most of the *in vitro*-grown accessions gave better AChE inhibitory activity than the field accessions (Table 1). One of the *in vitro*-grown accessions, Calcutta 4 (IC_{50}: 11.5 ± 6.1 µg/mL), gave a better activity than the reference standard eserine (IC_{50}: 31.2 ± 7.3 µg/mL).

3.4. Correlation among the antioxidative cuvette assays

The correlation among the antioxidant assays as determined by Pearson's coefficient r is shown in Table S-3. Different antioxidant assay methods (DPPH$^{\bullet}$ and FRAP) were employed in this study because it is assumed that more than one assay would reflect better the antioxidant potential of a complex mixture of secondary metabolites [57]. Each assay would also help to better know the mechanism of the antioxidant activity. The correlation of the antioxidant assays with the phytochemical composition among the field accessions was generally lower than the correlation among the *in vitro*-grown accessions (Table S-3 A). This is similar to the result obtained from the accessions tested in a previous study [26]. The result revealed a relatively good correlation between the DPPH$^{\bullet}$ and FRAP assays among both, the field ($r = 0.61$) and *in vitro* ($r = 0.66$) grown accessions. For the *in vitro*-grown samples, there was a strong correlation between TPC and DPPH$^{\bullet}$, and between TPC and FRAP, but a weak correlation between TFC and DPPH$^{\bullet}$. Teixeira et al. [58] also noticed a strong correlation between TPC and antioxidant assays in all their studied medicinal plants but a weak correlation between TFC and antioxidants. This indicates that other phenolic compounds apart from the flavonoids are responsible for the strong antioxidant capacity of the samples.

3.5. HPTLC method

For the first time, HPTLC was used to reveal the chemical fingerprint of *Musa* species field accessions in comparison with *in vitro*-grown accessions. Polar solvent systems were investigated due to prior information noted from the cuvette assay about the high phenolic content of the *Musa* spp accessions. Among the different mobile phases tested (Fig. S-5), a polar, acidic mobile phase comprising of ethyl acetate – toluene - formic acid – water (3.4: 0.5: 0.7: 0.5) gave the best separation and was used. The derivatization with the NP reagent revealed the fingerprint of phenolic compounds and flavonoids in the *Musa* spp. Phenolic compounds

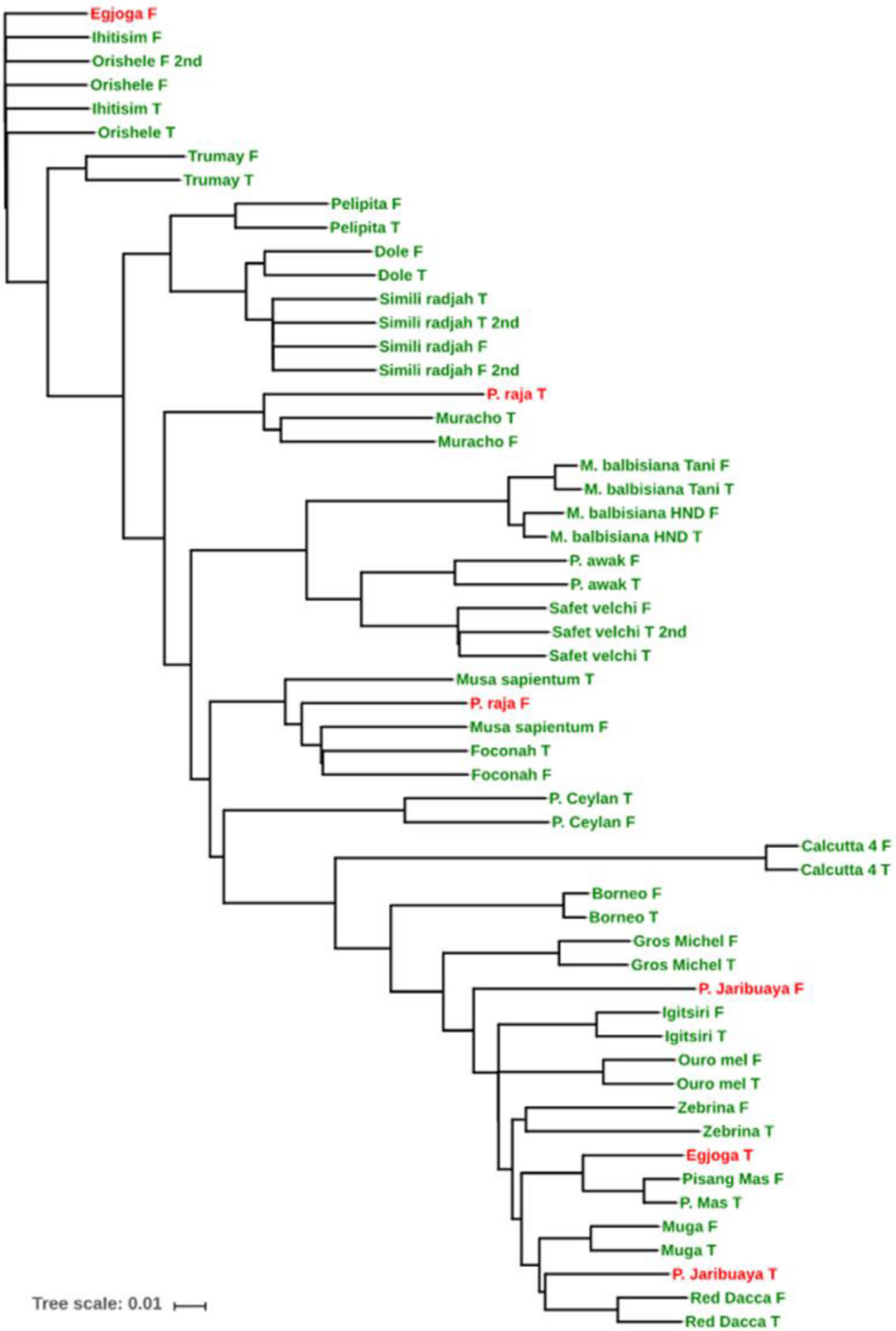

Fig. 1. Neighbor joining tree of field and *in vitro*-grown *Musa* spp. accessions using 150 k SNP markers.

are known to have a wide pharmacological activity range, such as antimicrobial [59], antioxidant [60], anti-inflammatory [61], antidiabetic [62], and antiulcer [63] properties among others. Phenolic compounds were found to be abundant from *in vitro*-grown samples (Fig. 2C). This is in support of the result obtained from the cuvette assay with the *in vitro* accessions giving higher TPC than the field-grown accessions. Also, the flavonoids shown as dark UV-absorbing bands at 254 nm and as green and orange fluorescent bands after derivatization in the NP reagent are seen in the field accessions, but not in the *in vitro*-grown accessions (Fig. 2C). Inter-

Table 1
Means ($n = 3$) of total phenolic content (TPC), flavonoid content (TFC), FRAP antioxidant potential, IC_{50} of $DPPH^{\bullet}$ free radical scavenging and AChE inhibitory activity of field-grown and *in vitro*-grown *Musa* spp. accessions.

No	Accession	Gen group	TPC (mg GAE/g)		TFC (mg QE/g)		FRAP (mg TE/g)		DPPH IC_{50} (μg/mL)		AChE IC_{50} (μg/mL)	
			Field	*In vitro*	Field	*In vitro*	Field	*In vitro*	Field	*In vitro*	Field	*In vitro*
1	P. Mas	AA	18.1 ± 2.7^{e}	72.1 ± 0.1^{c}	9.6 ± 3.1^{f}	3.4 ± 0.0^{f}	9.8 ± 1.5^{e}	53.3 ± 0.3 g	95.4 ± 0.7^{ef}	25.4 ± 2.1^{d}	**219.1 ± 13.8^{a}**	137.2 ± 23.8^{b}
2	Simili Radjah	ABB	**85.9 ± 1.4^{a}**	**124.5 ± 12.7^{a}**	30.3 ± 2.7^{b}	11.3 ± 0.7^{b}	18.8 ± 0.4^{b}	**140.3 ± 2.3^{b}**	**28.2 ± 1.3^{a}**	**10.7 ± 0.3^{a}**	610.6 ± 127.1^{c}	541.3 ± 81.1^{d}
3	Red Dacca	AAA	19.7 ± 3.1^{e}	38.5 ± 3.5^{e}	24.0 ± 1.7^{c}	3.8 ± 0.2^{e}	11.8 ± 0.9^{e}	102.4 ± 3.0^{c}	56.3 ± 1.8^{b}	25.1 ± 1.2^{d}	376.3 ± 40.2c	282.3 ± 59.8^{c}
4	Pelipita	ABB	14.4 ± 1.5^{ef}	21.7 ± 4.1^{f}	24.1 ± 1.8^{c}	2.5 ± 0.1 g	16.9 ± 0.5^{c}	27.7 ± 1.7^{i}	53.9 ± 0.5^{b}	46.9 ± 0.1^{f}	282.7 ± 19.4^{b}	429.0 ± 54.0^{d}
5	Safet Velchi	AABcv	33.6 ± 0.8^{c}	55.8 ± 3.7^{d}	3.6 ± 0.9^{h}	0.5 ± 0.3 g	11.3 ± 0.2^{e}	63.9 ± 0.9^{f}	78.8 ± 0.3^{d}	22.8 ± 0.6^{cd}	687.0 ± 26.1^{c}	1050.0 ± 274.1^{e}
6	Igitsiri	AAA	16.3 ± 0.8^{e}	43.0 ± 0.9^{cd}	9.4 ± 0.5^{f}	1.3 ± 0.1 g	16.2 ± 2.2^{c}	78.1 ± 2.4^{e}	65.5 ± 1.0^{c}	34.1 ± 1.0^{f}	430.8 ± 45.6^{c}	791.3 ± 36.1^{e}
7	Zebrina	AAwild	33.8 ± 0.1^{c}	56.3 ± 3.3^{d}	11.6 ± 0.3^{e}	1.6 ± 0.2 g	22.4 ± 2.0^{a}	52.3 ± 3.0 g	52.8 ± 0.1^{b}	17.9 ± 0.5^{bc}	419.0 ± 15.1^{c}	633.5 ± 71.8^{d}
8	Dole	ABB	7.6 ± 1.5 g	9.8 ± 0.2^{fg}	4.3 ± 0.2 g	0.6 ± 0.2 g	8.4 ± 1.2^{e}	22.9 ± 2.6^{i}	100.0 ± 2.2^{ef}	68.2 ± 1.6 g	2170.0 ± 372.9 g	771.5 ± 16.4^{e}
9	Foconah	AAB	34.6 ± 1.8^{c}	**87.5 ± 4.3^{b}**	11.4 ± 0.5^{e}	**14.6 ± 1.4^{a}**	14.6 ± 0.6^{d}	**152.2 ± 2.8^{a}**	56.2 ± 0.7^{b}	12.2 ± 0.8^{ab}	514.3 ± 90.3^{c}	289.4 ± 9.8^{c}
10	Gros Michel	AAA	**48.4 ± 1.4^{b}**	56.5 ± 0.7^{d}	**60.1 ± 6.3^{a}**	0.4 ± 0.1 g	8.6 ± 0.2^{e}	89.0 ± 0.2^{d}	101.4 ± 0.8^{f}	49.0 ± 0.8^{f}	1637.0 ± 253.1 g	434.6 ± 37.5^{d}
11	P. Ceylan	AAB	27.2 ± 2.5^{d}	76.3 ± 0.3^{bc}	28.7 ± 2.0^{c}	8.6 ± 0.2^{c}	5.7 ± 0.2^{f}	66.5 ± 0.9^{f}	257.9 ± 2.3^{i}	22.8 ± 0.5^{cd}	555.7 ± 17.8^{c}	420.9 ± 37.2^{d}
12	P. Jaribuaya	AA	29.2 ± 0.4^{cd}	66.9 ± 0.7^{cd}	11.1 ± 0.6^{e}	2.4 ± 0.6 g	23.8 ± 0.4^{a}	54.5 ± 2.2 g	92.2 ± 2.5^{e}	23.7 ± 0.2^{cd}	981.8 ± 62.6^{d}	494.0 ± 46.2^{d}
13	Calcutta 4	AAwild	32.9 ± 0.5^{c}	75.6 ± 2.4^{c}	4.2 ± 0.2 g	5.5 ± 0.7^{d}	4.3 ± 0.1^{f}	100.7 ± 3.5^{c}	148.4 ± 2.5 g	20.2 ± 0.2^{cd}	1124.0 ± 31.3^{e}	**11.5 ± 0.1^{a}**
14	M. balbi HND	BBwild	16.3 ± 1.1^{e}	19.6 ± 2.0^{f}	18.8 ± 2.6^{d}	1.1 ± 0.3 g	4.4 ± 0.7^{f}	32.4 ± 0.4^{h}	190.1 ± 11.2^{h}	116.4 ± 1.4^{h}	1280.0 ± 91.9^{f}	1181.0 ± 91.3^{e}
15	M. balbi Tani	BBwild	3.9 ± 0.4^{h}	2.4 ± 0.3 g	30.8 ± 2.8^{b}	1.1 ± 0.6 g	16.1 ± 0.5^{c}	10.6 ± 0.5^{j}	148.9 ± 5.5 g	154.4 ± 6.4^{i}	752.3 ± 45.3^{c}	780.4 ± 21.5^{e}

Means ($n = 3$) with the same letter in the same column are not significantly different at $P<0.05$. IC_{50} of gallic acid at 1.7 ± 0.0 μg/mL, ascorbic acid at 3.7 ± 0.1 μg/mL and serine at 31.2 ± 7.3 μg/mL.

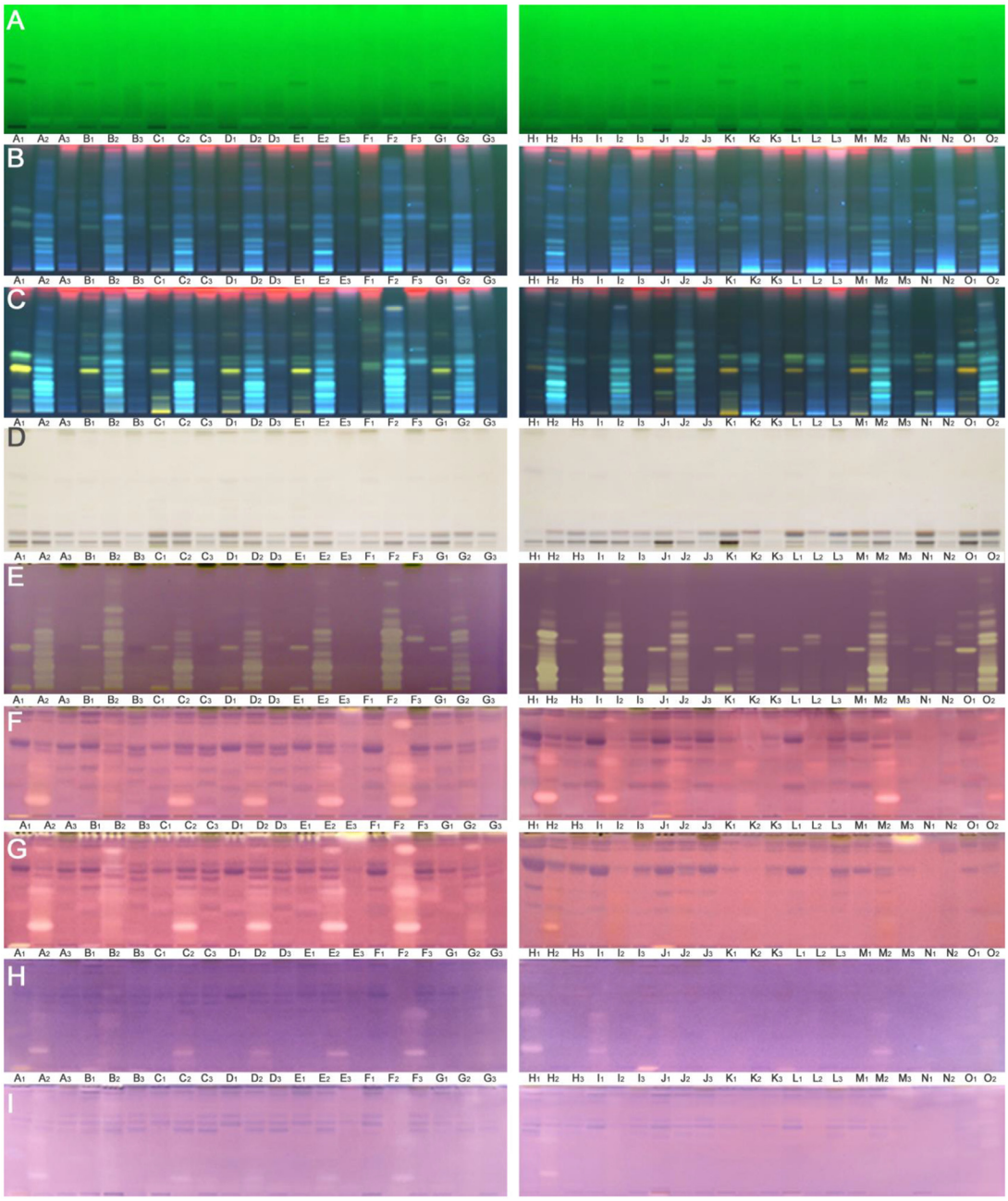

Fig. 2. HPTLC-UV/FLD-EDA fingerprints of field, *in vitro*-grown and acclimatized *Musa* spp. accessions (A1-O2 as assigned in Table S-1; 10 µL/band, except for AChE/BChE 25 µL/band) on silica gel HPTLC plates with ethyl acetate - toluene - formic acid – water, 3.4:0.5:0.7:0.5, documented (A) at UV 254 nm, (B) at UV 366 nm, (C) after derivatization using a reagent sequence starting with natural product reagent visualized at UV 366 nm, followed by ninhydrin reagent (no zones evident; not depicted) and lastly (D) diphenylamine reagent, (E) after derivatization by DPPH$^{\cdot}$ reagent as well as after (F) AChE, (G) BChE, (H) α-glucosidase and (I) β-glucosidase assays, all latter (E-I) documented at white light illumination.

estingly, this result is also in consonance with what was obtained previously from the cuvette assay. Field accessions gave higher total flavonoid content than the *in vitro*-grown accessions. The pattern obtained by derivatization with the DPA reagent is seen in Fig. 2D. Sugars were found in all samples when derivatized with this reagent selective for saccharides and glycosides. This underlines previous studies [64], in which sugars have been reported to be present in the leaves of *Musa* spp.

3.6. Effect-directed analysis by HPTLC-EDA

So far, the biological activities of *Musa* spp. such as antidiabetic activity of the fruit [65], anticholinesterase potential of the fruits and leaves [26] and antimicrobial activity of peel and leaf [14] have been reported using cuvette spectrophotometric assays and other *in vitro* and *in vivo* assays. For the first time, the present study shows the biological profiles of *Musa* spp. accessions using HPTLC-EDA. This work also compared the biological profiles of plants grown in different environments (field, *in vitro* and green house). The HPTLC-EDA helped to identify and observe clearly the compounds responsible for each biological activity, which is not possible with cuvette assays (sum parameter). In this study, HPTLC was hyphenated to DPPH$^{\bullet\cdot}$, AChE, BChE, α-glucosidase, β-glucosidase, α-amylase, *Aliivibrio fischeri, Bacillus subtilis* and *Salmonella thyphimurium* assays.

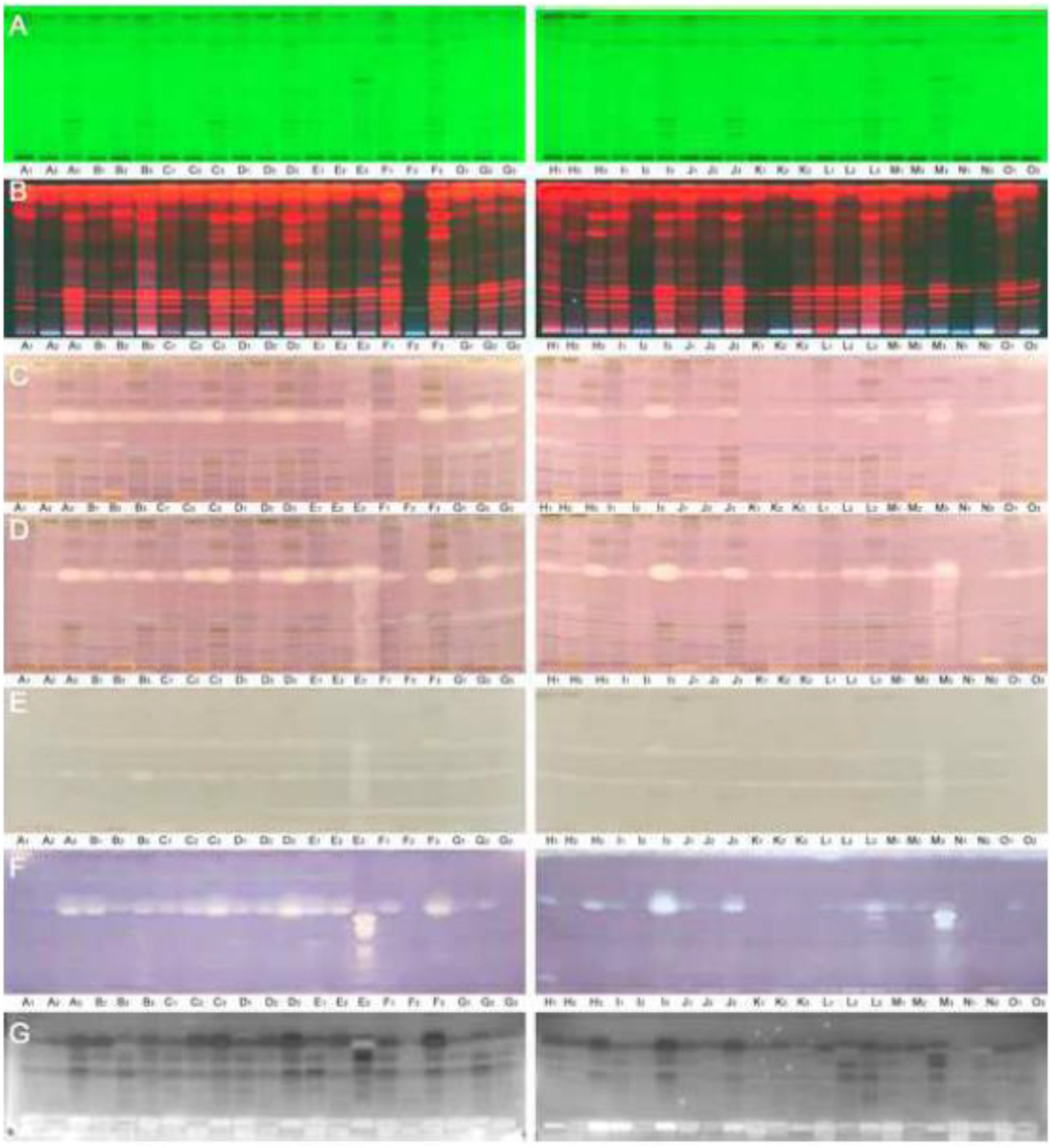

Fig. 3. HPTLC-UV/FLD-EDA fingerprints of field, *in vitro*-grown and acclimatized *Musa* spp. accessions (A1-O2 as assigned in Table S-1; 10 µL/band, except for AChE/BChE 15 µL/band) on silica gel HPTLC plates with toluene - ethyl acetate – methanol, 6:3:1, documented at (A) UV 254 nm, (B) UV 366 nm, and white light illumination after (C) AChE, (D) BChE, (E) α-amylase, (F) *B. subtilis*, and (G) *A. fischeri* assays.

3.6.1. Radical scavenging activity

The derivatization with the DPPH$^{\bullet}$ reagent revealed the presence of antioxidant compounds in *Musa* spp. as a pattern of whitish bands on a purple background (Fig. 2E). *In vitro*-grown accessions, which have many phenolic compounds, have many whitish radical scavenging bands unlike the field-grown accessions with flavonoids but reduced number and intensity of whitish zones. This joins the result of the correlation among the assays. The phenolic compounds are responsible for the antioxidant property of the plant samples, while the flavonoids contributed less. Similarly, the HPTLC-DPPH$^{\bullet}$ method revealed the variation in the chemical profile of samples from different origin with different genome group. Just like the result obtained from the cuvette spectrophotometric assays, the samples with the high TPC, TFC, DPPH$^{\bullet}$ and FRAP values also have many whitish radical scavenging bands after derivatization with the DPPH$^{\bullet}$ reagent, while samples with low cuvette assay values have fewer bands (Fig. 2E). *In vitro* grown accessions gave the highest peak area values of the radical scavenging compounds (Table S-4). These *in vitro*-grown accessions that are rich in phenolics and antioxidants can be explored for natural products isolation.

3.6.2. Detection of AChE and BChE inhibitors

Compounds that can inhibit cholinesterase enzymes were found in the *Musa* spp. accessions tested (Figs. 2 and 3). Cholinesterase inhibitors are known to be important drugs for treating neurological disorders such as Alzheimer's diseases. Key enzymes found in the human neurological system are AChE and BChE. For example, AChE is responsible for the breakdown of acetylcholine into choline and acetic acid, which leads to the reduction in the acetylcholine level in the body [66]. The body has a way of balancing the situation, but in disease condition, a cholinesterase inhibitor is usually needed. Plants containing AChE and BChE inhibitors are good sources of neurodegenerative diseases drug development [67].

The AChE and BChE inhibitors are seen as white bands on a purple background. With the polar, acidic mobile phase (ethyl ac-

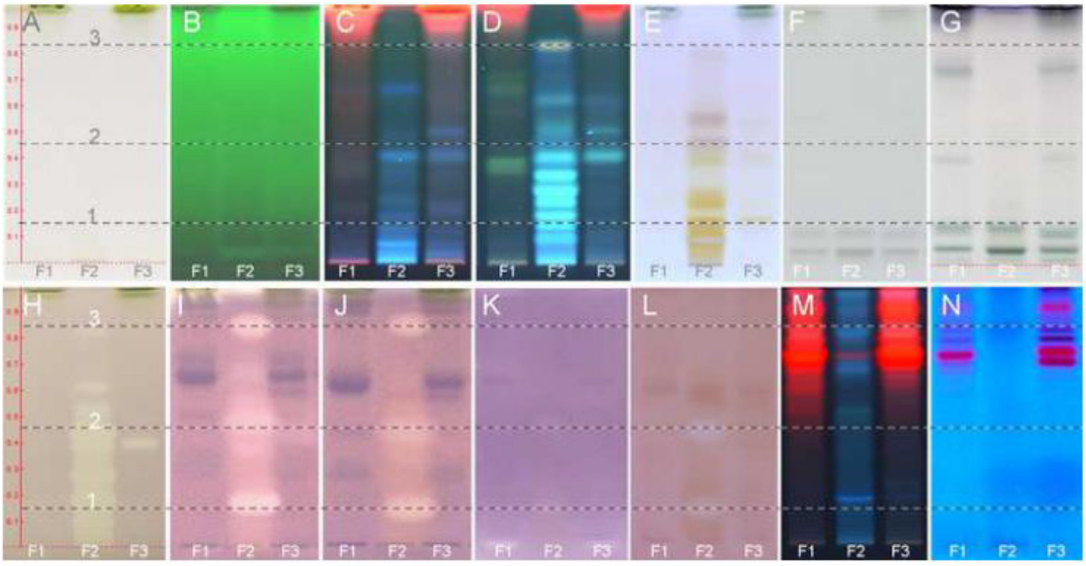

Fig. 4. Detailed comparison of active compounds 1–3 in the HPTLC fingerprints (as in Fig. 2) for *Musa* spp. leaf extract F1-F3, detected at (A) white light illumination (B) UV 254 nm, (C) UV 366 nm, (D) after derivatization using a reagent sequence starting with natural product reagent at 366 nm, followed by (E) ninhydrin reagent and lastly (F) diphenylamine reagent, (G) after derivatization with *p*-anisaldehyde, (H) DPPH• as well as after (I) AChE, (J) BChE, (K) α-glucosidase, and (L) β-glucosidase inhibition assays; same applied (15 µL/band) on HPTLC RP18 W plate (M) at UV 366 nm and (N) after genotoxicity assay at UV 366 nm.

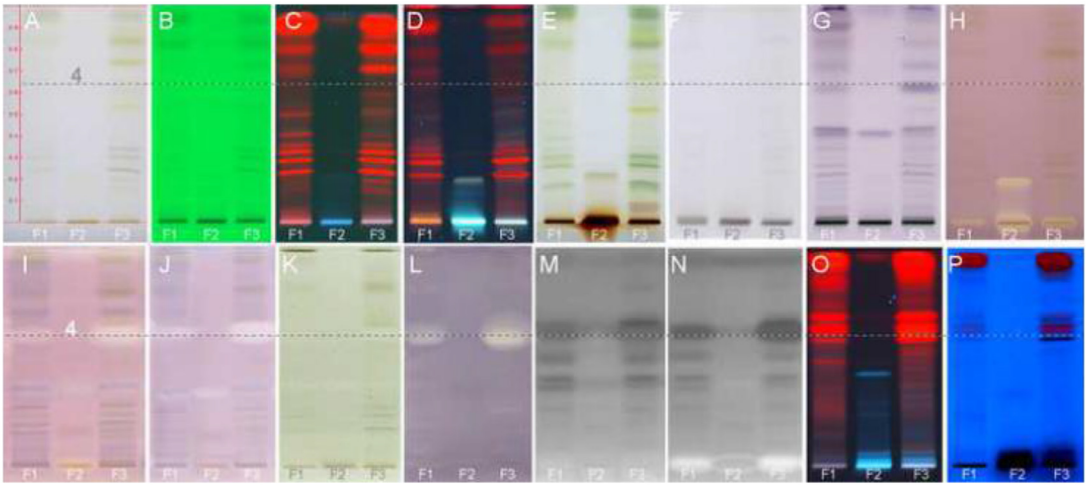

Fig. 5. Detailed comparison of active compound 4 in the HPTLC fingerprints (as in Fig. 3) for *Musa* spp. leaf extract F1-F3, detected (A) at white light illumination (B) at UV 254 nm, (C) at UV 366 nm, after derivatization using a reagent sequence (D) starting with natural product reagent at 366 nm, followed by (E) ninhydrin reagent and lastly (F) diphenylamine reagent, (G) after derivatization with *p*-anisaldehyde, (H) DPPH• as well as after (I) AChE, (J) BChE, (K) α-amylase inhibition assays, all latter documented at white light illumination, and after bioassays (L) *B. subtilis* and (M) *A. fischeri* after 3 min and (N) 30 min (both as bioluminescence image); same applied (15 µL/band) on HPTLC RP18 W plate (O) at UV 366 nm and (P) after genotoxicity assay at UV 366 nm.

etate – toluene - formic acid – water, 3.4: 0.5: 0.7: 0.5), three major compounds (Fig. 4) at hR_F values 15, 44 and 83 were identified as AChE and BChE inhibitors and were observed from *in vitro*-grown accessions. White bands were noticed at the solvent front so the elution power was reduced. With the medium polar mobile phase (toluene – ethyl acetate – methanol, 6:3:1), one major compound (Fig. 5) with hR_F 63 was identified to inhibit AChE and BChE in almost all the samples tested with higher band intensity in the acclimatized accessions. In some samples (I to O, except J1 on start zone and M3 in front), no inhibitor compounds were detected when the polar mobile phase was used, suggesting that those samples do not contain any BChE inhibitory compound (Fig. 2).

3.6.3. Detection of α-/β-glucosidase and α-amylase inhibitors

The inhibition of α-glucosidase, β-glucosidase and α-amylase is linked to the antidiabetic effect. These three enzymes are found in the digestive system. They are responsible for the breakdown of carbohydrates to glucose thereby increasing the blood glucose level in diabetes patients. The inhibition of these enzymes plays an important role in the management of diabetes, reducing the hydrolysis of carbohydrates [68,69]. HPTLC combined with glucosidase assays revealed compounds with α-glucosidase and β-glucosidase inhibitory activity in the tested *Musa* spp. accessions. Two major compounds were identified from *in vitro*-grown accessions when the polar, acidic mobile phase (ethyl acetate – toluene - formic acid - water, 3.4: 0.5: 0.7: 0.5) was used. They appeared as white bands on a purple background (Fig. 2H and I). Some of the accessions: Pelipita (J), *M. balbisiana* Tani (K), Dole (L), *M. balbisiana* HND (N) and Igitsiri (O) did not show any inhibition zones in both α- and β-glucosidase assays, and similar results were observed in the cholinesterase assay. The zones of inhibition for the field-grown and acclimatized accessions were seen at the appli-

Table 2
HPTLC-HRMS data of bioactive compounds in the selected samples F_2 and F_3.

Sample	Com-pound	hR_F	Observed mass (*m/z*)	Assignment	Molecular formula	Mass error (ppm)	Intensity	Formula	Potential candidate (s)
F_2	1	15	131.0461	$[M\text{-}H]^-$	$C_4H_7O_3N_2$	7.78	5.89E+07	$C_4H_8O_3N_2$	asparagine
			133.0606	$[M+H]^+$	$C_4H_9O_3N_2$	1.343	9.26E+08		
	2	44	146.966	$[M\text{-}H]^-$			9.13E+07	$C_9H_{11}NO_2$	4-aminohydrocinnamic acid, phenylalanine, 2-amino-3,4-dimethylbenzoic acid, 2-(4-methylphenoxy) acetamide
			166.0866	$[M+H]^+$	$C_9H_{12}NO_2$	1.956	5.61E+08		
	3	83	218.0823	$[M\text{-}H]^-$	$C_{12}H_{12}O_3N$	4.632	1.90E+08	$C_{12}H_{13}O_3N$	pyrrolidinone, aniracetam
			437.1717	$[2M\text{-}H]^-$			5.62E+07		
			242.0783	$[M+Na]^+$	$C_{12}H_{13}O_3NNa$	1.754	2.95E+08		
			461.1676	$[2M+Na]^+$			6.04E+07		
F_3	4	63	277.2175	$[M2\text{-}H]^-$	$C_{18}H_{29}O_2$	2.795	1.38E+08	$C_{18}H_{30}O_2$	linolenic acid
			301.2132	$[M2+Na]^+$			1.84E+07		
			171.1028	$[M\text{-}H]^-$	$C_9H_{15}O_3$	4.154	1.21E+08	$C_9H_{15}O_3$	
			195.099	$[M+Na]^+$	$C_9H_{16}O_3Na$	4.377	7.50E+07		

cation zone when the polar, acidic mobile phase was used. As a white shimmering was noticed at the solvent front (Fig. S-6A), further less polar mobile phases were tested and revealed further inhibition zones (Fig. S-6C). For α-amylase, a clear inhibition zone was detected at the solvent front for sample E3 (Zebrina, Fig. S-6E), whereas for other samples, the white shimmering at the solvent front was weaker. In order to reduce the elution power, the medium polar mobile phase was tested. This revealed two zones of inhibition, at hR_F 40 and 63, which were in all samples more or less intense (Fig. 3E).

3.6.4. Detection of antimicrobials

There are several reports on the antimicrobial properties of different parts of *Musa* spp. using agar well diffusion assay [70,71], but for the first time, the inhibition of these microorganisms was reported via HPTLC-EDA analysis. The HPTLC-*B. subtilis* bioassay (Gram-positive bacteria) revealed one main antibacterial zone (hR_F 63) with a very intense band in almost all the samples (Figs. 3F and 5L). The acclimatized samples gave more intense bands. *M. balbisiana* Tani, Dole, *M. balbisiana* HND and Igitsiri were the accessions with weak or no inhibition zones (Fig. 3F). For the HPTLC-*Aliivibrio fischeri* bioassay (Gram-negative bacteria), antimicrobials were detected based on their impact on the bioluminescence (metabolic activity) of *A. fischeri* bacteria, appearing as dark (inhibiting) or bright (enhancing) zones on an instantly luminescent bacterial plate background. Many dark zones of inhibition were observed in the different *Musa* spp. accessions (Fig. 3G) with increasing intensity as the time increased.

3.6.5. Absence of genotoxins

The HPTLC-genotoxicity assay via *Salmonella thyphimurium* bacteria (SOS-Umu-C bioassay) [47] applied to the plant samples showed that the *Musa* spp. contained no genotoxic compounds for the given highest amount of 38 µg methanolic extract applied (15 µL/band of a 2.5 mg/mL solution, Fig. S-7). The toxic positive control 4-nitroquinoline-1-oxide appeared as blue fluorescence at UV 366 nm, while the samples even at a higher amount on the plate gave no such fluorescence after development with both mobile phases (Fig. S-7). *In vivo* animal model studies have been used to report the toxicity profile of some parts of *Musa paradisiaca* L. The juice from the pseudostem of *Musa paradisiaca* was reported to be non-toxic [72]. The ethanol extract of the leaf was found to be slightly toxic with an LD_{50} of 490 mg/kg body weight of the mice [70], while the unripe fruit extract was non-toxic and safe for pharmaceutical use [73]. These findings support our results. In HPTLC, still higher sample volumes can be analyzed to lower the detectability, but was not performed in this study.

3.7. Characterization of active zones via HPTLC-HRMS

The multipotent active zones were characterized by HPTLC-HRMS after online elution via an elution head-based interface. The multipotent compounds 1 to 3 were obtained from only *in vitro* grown accessions developed in the polar, acidic mobile phase (Fig. 4). The band of compound 3 was very intense *in vitro*-grown Calcutta 4 (F_2), but was not visible or absent in some accessions (*M. balbisiana* Tani, Dole and *M. balbisiana* HND). Calcutta 4 field (F_1), *in vitro* (F_2) and acclimatized extracts (F_3) were considered as representative samples based on the HPTLC-EDA assay results. The following tentative assignment of the compounds was based on the respective base peak in the HPTLC-HRMS spectrum, HPTLC derivatization and literature data (Table 2).

Compound 1 (hR_F 15) which is a blue fluorescent compound at UV 366 nm (Fig. 4) gave a base peak at *m/z* 133.0606, which was assigned as $[M+H]^+$ (Fig. 6) with $C_4H_9O_3N_2$ as calculated molecular formula. The sodium adduct was seen at *m/z* 155.0424 $[M+Na]^+$ ($C_4H_8O_3N_2Na$). In the negative mode, the base peak at *m/z* 131.0461, assigned as $[M\text{-}H]^-$ ($C_4H_7O_3N_2$), underlined the previous result. Thus, the actual molecular formula of compound 1 was preliminary assigned to be $C_4H_8O_3N_2$. This molecular formula fit to an amino acid (different forms of asparagine, alanine and glycine anhydride). Though aspartic acid and other amino acids have been reported to be present in the pulp [74] and peel [75] of *Musa* spp., further experiments (selectivity of the mobile phase needs to be adjusted) are needed to clarify the observed effects. Compound 1 showed strong radical scavenging (antioxidant) activity and strong AChE and BChE inhibition, but moderate α- and β-glucosidase inhibition based on the HPTLC-EDA results (Fig. 4).

Compound 2 (hR_F 44) showed a characteristic blue color after derivatization with the NP reagent. It showed the same effects as compound 1. The base peak at *m/z* 166.0866 was assigned to be $[M+H]^+$ with $C_9H_{12}NO_2$ as molecular formula. In the negative mode, the respective base peak $[M\text{-}H]^-$ was at *m/z* 146.9660. Thus, the formula of compound 2 ($C_9H_{11}NO_2$) corresponds to that of a simple aromatic ring (benzene) with an amino group, carbonyl and hydroxyl group attached which could be 4-aminohydrocinnamic acid, phenylalanine, 2-amino-3,4-dimethylbenzoic acid or 2-(4-methylphenoxy) acetamide.

Compound 3 (hR_F 83) was not UV sensitive and gave a characteristic yellow color surrounded by blue color after derivatization in NP reagent (Fig. 4). In the positive ionization mode, the recorded mass spectra of this zone showed a base peak at *m/z* 242.0783, which was assigned as $[M+Na]^+$ ($C_{12}H_{13}O_3NNa$). The dimer of this compound was seen at *m/z* 461.1676 and assigned as $[2M+Na]^+$ (Fig. 6). In the negative mode, the respective base peak was at *m/z*

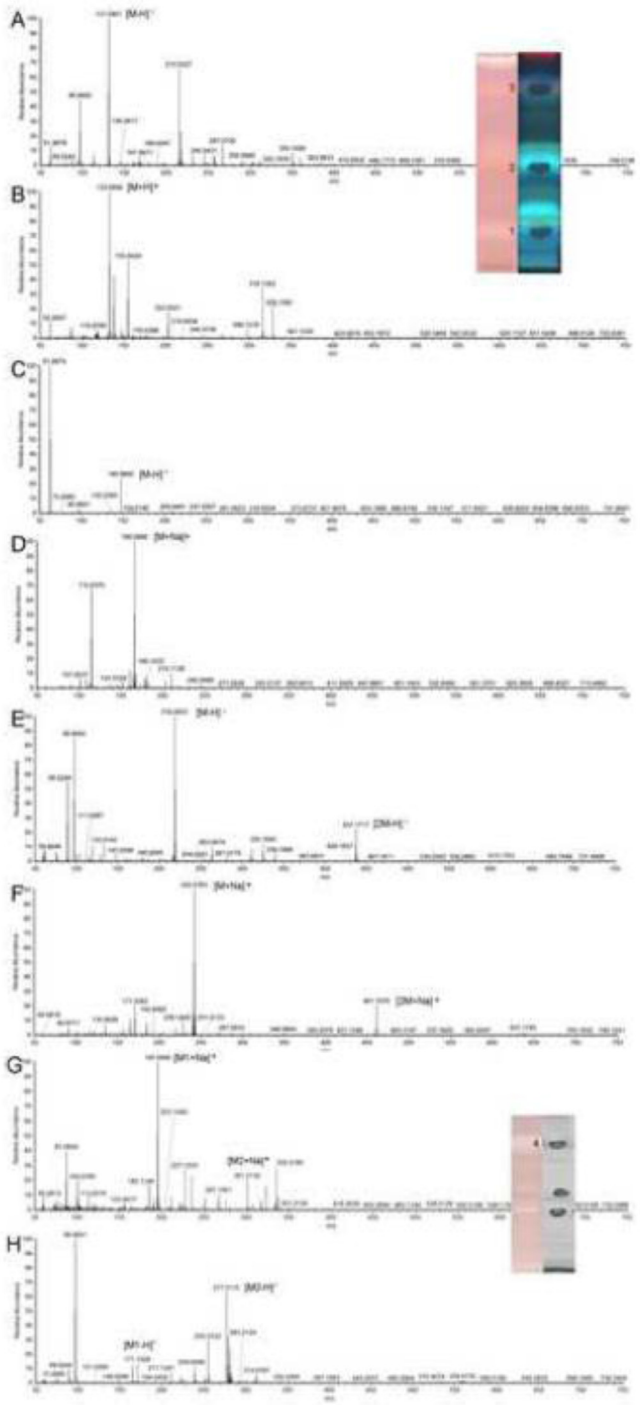

Fig. 6. HPTLC-HRMS spectra of compounds 1–3 in sample extract F_2 (A-F; conditions as in Fig. 3, 25 µL/band) and compound 4 in sample extract F_3 (G and H; conditions as in Fig. 4; 15 µL/band); for zone marking, a plate stripe was supplied to the AChE assay, and after zone elution, the plate stripe was immersed into a suited derivatization reagents to check proper positioning.

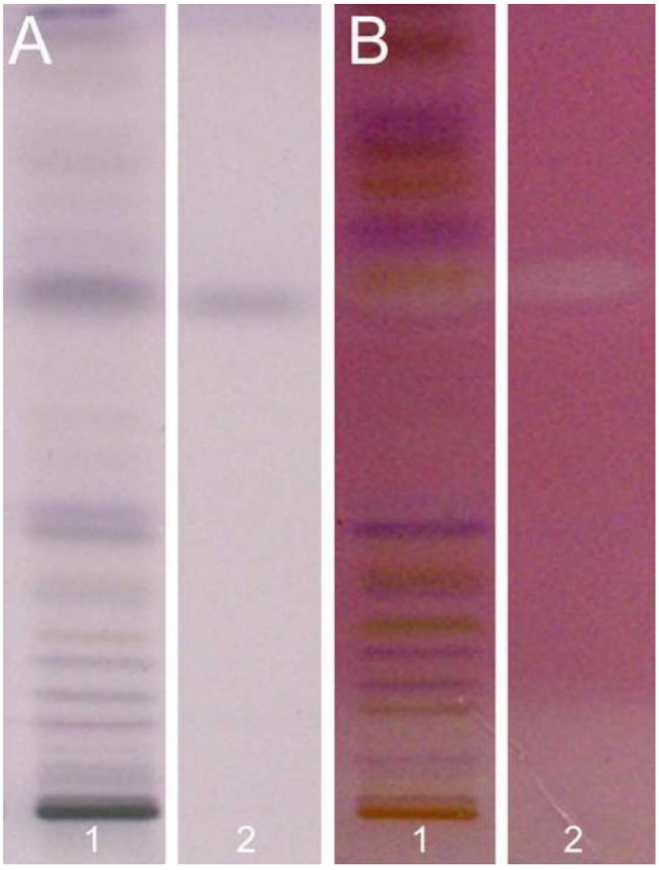

Fig. 7. Co-chromatography of sample extract F_4, track 1 (10 µL/band), standard linolenic acid, track 2 (100 ng/µL, 0.1 mg/ml methanol, 5 µL applied) confirmed compound 4 to be linolenic acid (A) derivatized in *p*-anisaldehyde reagent and (B) after AChE assay.

218.0823 $[M-H]^-$ with its dimer $[2M-H]^-$ at *m/z* 437.1717. Thus, the actual molecular formula of this compound was $C_{12}H_{13}O_3N$. From literature, this compound was found to be an alkaloid with a pyrrolidine base. It is most likely aniracetam. Pyrrolidine alkaloids are used as anticholinergic drugs. Based on the HPTLC-EDA results, compound 3 showed a moderate antioxidant activity, a very strong AChE and BChE, but no α- and β-glucosidase inhibition. Many alkaloids from plants such as rivastigmine, galantamine and huperzine A have been reported for their anticholinesterase activity [76,77]. In *Musa* spp. and in Musaceae family, pyrrolidine alkaloids have not been reported so far and this suggested preliminary assignment is new.

The multipotent compound 4 (hR_F 63) was present in all the samples and abundant in acclimatized accessions based on the peak area. It was obtained from sample extract F_3 developed in the medium polar mobile phase (Fig. 5). Compound 4 showed a characteristic purple color when derivatized with the *p*-anisaldehyde reagent. The mass spectra of this zone showed a base peak at *m/z* 277.2175, which was assigned as $[M-H]^-$ with the formula $C_{18}H_{29}O_2$. In the positive mode, the respective sodium adduct of this compound was seen at *m/z* 301.2132. Other unassigned fragments were also seen (Fig. 6G and H). The actual molecular formula of this compound was found to be $C_{18}H_{30}O_2$, indicating linolenic acid (octadeca-9,12,15-trienoic acid). By co-chromatography of the sample and the standard (Fig. 7), compound 4 was confirmed to be linolenic acid. This fatty acid has been reported to be present in the fruits of different *Musa* spp. cultivars [78] also in the leaves [21]. This polyunsaturated fatty acid is an essential fatty acid that cannot be synthesized by the human body and therefore, must be supplied by external sources. *Musa* spp. is shown to be an excellent source of this fatty acid. In this study, this fatty acid is reported to have multiple bioactivities. It showed strong AChE, BChE, *B. subtilis* and *A. fischeri* inhibitory properties, but a weak α-amylase inhibition and no radical scavenging (antioxidant) activity. These multiple bioactivities of linolenic acid were confirmed in parallel studies on *Primula* species in our group [79].

Conclusions

This study for the first time provided the chemical, enzymatic and biological fingerprints of *Musa* spp. using hyphenated HPTLC. Up to 22 samples were simultaneously analyzed within a short time. It presented a simple, fast and streamlined workflow for the detection and characterization of multipotent secondary metabolites in *Musa* spp. This straightforward hyphenation helped to detect, characterize and even identify individual bioactive compounds in the complex extracts. The results of the HPTLC-EDA analysis confirmed the sum parameter results obtained by spectrophotometric cuvette assays. The samples with an overall high TPC and antioxidant activity were also seen to have many antioxidative bands with high peak area signals, while the samples with low TPC and antioxidant activity were seen to have fewer bands in many of the HPTLC-EDA autograms. The *in vitro*-grown accessions had the best antioxidant property and contained compounds 1 to 3, which were not detected in the field and the acclimatized samples. Compound 4 (linolenic acid) was found in all the samples, but was abundant in acclimatized accessions. This study confirmed the use of *Musa* spp. tissue cultures as an alternative mean of plant material supply for the pharmaceutical industry and demonstrated a suitable bioanalytical tool for activity control.

Author contributions

I. Ayoola-Oresanya did most experiments (partly done by master student N. Hockamp at JLU Giessen) and wrote the manuscript draft, revised by all authors except for R. Paliwal. M. Sonibare supervised the UV-spectrophotometric assays. B. Gueye supervised the *in vitro* cultivation, R. Paliwal did the DNA sequence analysis, M. Abberton organized the SNP sequencing, and G. Morlock supervised the HPTLC research performed at JLU Giessen.

Declaration of Competing Interest

The authors declare that they have no known competing financial interests or personal relationships that could have appeared to influence the work reported in this paper.

The authors declare no conflict of interest.

Acknowledgments

This work was supported by the German Academic Exchange Service, Germany (DAAD) short-term grant given to I. Ayoola-Oresanya for her stay at JLU Giessen. The authors are grateful to the Food Science group at JLU Giessen for assistance, especially to N. Hockamp. Instrumentation was partially funded by the Deutsche Forschungsgemeinschaft (DFG, German Research Foundation) - INST 162/471-1 FUGG; INST 162/536-1 FUGG.

Supplementary materials

Supplementary material associated with this article can be found, in the online version, at doi:10.1016/j.chroma.2019.460774.

References

[1] I. Choma, W. Jesionek, TLC-direct bioautography as a high throughput method for detection of antimicrobials in plants, Chromatography 2 (2015) 225–238.
[2] G.E. Morlock, Instrumental methods for the analysis and identification of bioactive molecules, in: ACS Symposium Series, 1185, 2013, pp. 101–121, doi:10.1021/bk-2014-1185.ch005.
[3] M. Jamshidi-Aidji, G.E. Morlock, From bioprofiling and characterization to bioquantification of natural antibiotics by direct bioautography linked to high-resolution mass spectrometry: exemplarily shown for salvia miltiorrhiza root, Anal. Chem. 88 (2016) 10979–10986, doi:10.1021/acs.analchem.6b02648.
[4] Á.M. Móricz, P.G. Ott, G.E. Morlock, Discovered acetylcholinesterase inhibition and antibacterial activity of polyacetylenes in tansy root extract via effect-directed chromatographic fingerprints, j, Chromatogr. A. 1543 (2018) 73–80, doi:10.1016/j.chroma.2018.02.038.
[5] T. Müller, S. Vergeiner, B. Kräutler, Structure elucidation of chlorophyllcatabolites (phyllobilins) by ESI-mass spectrometry – pseudo-molecular ionsand fragmentation analysis of a nonfluorescent chlorophyll catabolite (NCC), Int. J. Mass Spectrom. 365–366 (2014) 48–55.
[6] I. Yüce, G.E. Morlock, Streamlined structure elucidation of an unknown compound in a pigment formulation, J. Chromatogr. A. 1469 (2016) 120–127, doi:10.1016/j.chroma.2016.09.040.
[7] H. Luftmann, M. Aranda, G.E. Morlock, Automated interface for hyphenationof planar chromatography with mass spectrometry, Rapid Commun. MassSpectrom. 21 (2007) 3772–3776.
[8] G. Morlock, W. Schwack, Hyphenations in planar chromatography, J.Chromatogr. A 1217 (2010) 6600–6609.
[9] W.H. Perera Córdova, S.G. Leitão, G. Cunha-Filho, R.A. Bosch, I.P. Alonso, R. Pereda-Miranda, R. Gervou, N.A. Touza, L.E.M. Quintas, F. Noël, Bufadienolidesfrom parotoid gland secretions of Cuban toad Peltophryne fustiger(Bufonidae): inhibition of human kidney Na+/K+-ATPase activity, Toxicon 110 (2016) 27–34.
[10] E.O. Adewoye, V.O. Taiwo, F.A. Olayioye, Anti-oxidant and anti-hyperglycemic activities of *Musa sapientum* root extracts in alloxan-induced diabetic rats, Afr. J. Med. Med. Sci. 38 (2009) 109–117.
[11] P.K. Agarwal, A. Singh, K. Gaurav, S. Goel, H.D. Khanna, R.K. Goel, Evaluation of wound healing activity of extracts of plantain banana (Musa sapientum var. paradisiaca) in rats, Indian J. Exp. Biol. 47 (2009) 322–340.
[12] K.P.S. Kumar, D. Bhowmik, S. Duraivel, M. Umadevi, Traditional and medicinal uses of banana, J. Pharmacog. Phytochem. 1 (2012) 51–63.
[13] J.A.O. Ojewole, C.O. Adewunmi, Hypoglycemic effect of methanolic extract of Musa paradisiaca (Musaceae) green fruits in normal and diabetic mice, Methods Find. Exp. Clin. Pharmacol. 25 (2003) 453–456.
[14] C.S. Alisi, C.E. Nwanyanwu, C.O. Akujobi, C.O. Ibegbulem, Inhibition of dehydrogenase activity in pathogenic bacteria isolates by aqueous extracts of Musa paradisiaca (Var Sapientum), Afr. J. Biotechnol. (2008) 7.
[15] M.R. Zuzarte, A.M. Dinis, C. Cavaleiro, L.R. Salgueiro, J.M. Canhoto, Trichomes, essential oils and *in vitro* propagation of Lavandula pedunculata (Lamiaceae), Ind. Crops Prod. 32 (2010) 580–587.
[16] S. Ramachandra Rao, G.A. Ravishankar, Plant cell cultures: chemical factories of secondary metabolites, Biotechnol. Adv. 20 (2002) 101–153, doi:10.1016/S0734-9750(02)00007-1.
[17] N.D. Salvi, L. George, S. Eapen, Plant regeneration from leaf base callus of turmeric and random amplified polymorphic DNA analysis of regenerated plants, Plant Cell. Tissue Organ Cult. 66 (2001) 113–119.
[18] R.K. Sahaa, S. Acharyaa, S.S.H. Shovon, P. Royb, Medicinal activities of the leaves of Musa sapientum var. sylvesteris *in vitro*, Asian Pac. J. Trop. Biomed. 3 (6) (2013) 476–482.
[19] H.V. de Vasconcelos Facundo, D. dos Santos Garruti, C.T. dos Santos Dias, B.R. Cordenunsi, F.M. Lajolo, Influence of different banana cultivars on volatile compounds during ripening in cold storage, Food Res. Int. 49 (2012) 626–633.
[20] C. Vilela, S.A.O. Santos, J.J. Villaverde, L. Oliveira, A. Nunes, N. Cordeiro, C.S.R. Freire, A.J.D. Silvestre, Lipophilic phytochemicals from banana fruits of several Musa species, FoodD Chem 162 (2014) 247–252, doi:10.1016/j.foodchem.2014.04.050.
[21] M.A. Sonibare, I.O. Ayoola, B. Gueye, M.T. Abberton, R. D'Souza, N. Kuhnert, Leaves metabolomic profiling of Musa acuminata accessions using UPLC – QTOF – MS / MS and their antioxidant activity, J. Food Meas. Charact. (2018), doi:10.1007/s11694-018-9725-4.
[22] C.A. Cruz-cruz, G. Ramírez-tec, K. García-sosa, F. Escalante-erosa, L. Hill, A.E. Osbourn, L.M. Peña-rodríguez, Phytoanticipins from banana (Musa acuminata cv . Grande Naine) plants, with antifungal activity against Mycosphaerella fijiensis, the causal agent of black Sigatoka, (2010) 459–463. doi:10.1007/s10658-009-9561-9.
[23] N.S. Mathew, P.S. Negi, Traditional uses, phytochemistry and pharmacology of wild banana (Musa acuminata Colla): a review, J. Ethnopharmacol 196 (2017) 124–140.
[24] C.B. Bonnet, O. Hubert, D. Mbeguie-a-mbeguie, D. Pallet, A. Hiol, M. Reynes, P. Poucheret, Effect of physiological harvest stages on the composition of bioactive compounds in Cavendish bananas, J. Zhejiang Univ. Sci. B 14 (2013) 270–278, doi:10.1631/jzus.B1200177.
[25] B. Gueye, A. Adeyemi, M. Debiru, B. Akinyemi, M. Olagunju, A. Okeowo, S. Otukpa, D. Dumet, Standard Operation Procedures (SOP) For IITA *in Vitro* Genebank, IITA, Nigeria, 2012.
[26] I.O. Ayoola, B. Gueye, M.A. Sonibare, M.T. Abberton, Antioxidant activity and acetylcholinesterase inhibition of field and *in vitro* grown Musa L. species, J. Food Meas. Charact. 11 (2017) 488–499, doi:10.1007/s11694-016-9416-y.
[27] T. Murashige, F. Skoog, A revised medium for rapid growth and bio assays with tobacco tissue cultures, Physiol. Plant. 15 (1962) 473–497.
[28] J.J. Doyle, Isolation of plant DNA from fresh tissue, Focus (Madison) 12 (1990) 13–15.
[29] K. Shankar, L. Chavan, S. Shinde, B. Patil, An improved DNA extraction protocol from four *in vitro* banana cultivars, Asian J. Biotechnol. 3 (2011) 84–90.
[30] P. Wenzl, J. Carling, D. Kudrna, D. Jaccoud, E. Huttner, A. Kleinhofs, A. Kilian, Diversity arrays technology (DArT) for whole-genome profiling of barley, Proc. Natl. Acad. Sci. 101 (2004) 9915–9920.

[31] P.J. Bradbury, Z. Zhang, D.E. Kroon, T.M. Casstevens, Y. Ramdoss, E.S. Buckler, TASSEL: software for association mapping of complex traits in diverse samples, Bioinformatics 23 (2007) 2633–2635.
[32] R.C. Team, R: a language and environment for statistical computing, (2013).
[33] M. Khatoon, E. Islam, R. Islam, A.A. Rahman, A.H.M.K. Alam, P. Khondkar, M. Rashid, S. Parvin, Estimation of total phenol and *in vitro* antioxidant activity of Albizia procera leaves, BMC Res. Notes. 6 (2013) 1, doi:10.1186/1756-0500-6-121.
[34] H. Fathi, M.A. Ebrahimzadeh, Antioxidant and free radical scavenging activities of Hypericum perforatum L.(st. John's wort), Int. J. For. Soil Eros. 3 (2013) 68–72.
[35] D. Susanti, H.M. Sirat, F. Ahmad, R.M. Ali, N. Aimi, M. Kitajima, Antioxidant and cytotoxic flavonoids from the flowers of Melastoma malabathricum L, Food Chem. 103 (2007) 710–716.
[36] K.H. Musa, A. Abdullah, K. Jusoh, V. Subramaniam, Antioxidant activity of pink-flesh guava (Psidium guajava L.): effect of extraction techniques and solvents, Food Anal. Method. 4 (2011) 100–107.
[37] G.L. Ellman, K.D. Courtney, V. Andres Jr, R.M. Featherstone, A new and rapid colorimetric determination of acetylcholinesterase activity, Biochem. Pharmacol. 7 (2) (1961) 88–95.
[38] T.O. Elufioye, E.M. Obuotor, A.T. Sennuga, J.M. Agbedahunsi, S.A. Adesanya, Acetylcholinesterase and butyrylcholinesterase inhibitory activity of some selected Nigerian medicinal plants, Rev. Bras. Farmacogn. 20 (4) (2010) 472–477.
[39] E. Azadniya, G.E. Morlock, Bioprofiling of salvia miltiorrhiza via planar chromatography linked to (bio)assays, high resolution mass spectrometry and nuclear magnetic resonance spectroscopy, J. Chromatogr. A. 1533 (2018) 180–192, doi:10.1016/j.chroma.2017.12.014.
[40] M. Jamshidi Aijdi, J. Macho, M. Müller, G.E. Morlock, Effect-directed profiling of aqueous, fermented plant preparations via high-performance thin-layer chromatography combined with *in situ* assays and high-resolution mass spectrometry, J. Liq. Relat. Techn. (2019) 1–8.
[41] Á.M. Móricz, M. Jamshidi-Aidji, D. Krüzselyi, A. Darcsi, A. Böszörményi, P. Csontos, S. Béni, P.G. Ott, G.E. Morlock, Distinction and valorization of 30 root extracts of five goldenrod (Solidago) species, J. Chromatogr. A. (2019) in print.
[42] M. Jamshidi-Aidji, G.E. Morlock, Bioprofiling of unknown antibiotics in herbal extracts: development of a streamlined direct bioautography using *Bacillus subtilis* linked to mass spectrometry, J. Chromatogr. A. 1420 (2015) 110–118.
[43] A. Marston, Thin-layer chromatography with biological detection inphytochemistry, J. Chromatogr. A 1218 (2011) 2676–2683.
[44] S. Krüger, O. Urmann, G.E. Morlock, Development of a planarchromatographic method for quantitation of anthocyanes in pomace, feed,juice and wine, J. Chromatogr. A 1289 (2013) 105–118 http://dx.doi.org/10.1016/j.chroma.2013.03.005.
[45] European Committee for Standardization, Water quality – Determination ofthe inhibitory effect of water samples on the light emission of Vibrio fischeri(Luminescent bacteria test) DIN EN ISO 11348-1:2009–05 (2009).
[46] A.A. Bulich, Use of luminescent bacteria for determining toxicity in aquaticenvironments ASTM International, in: Aquatic Toxicology: Proceedings of the Second Annual Symposium on Aquatic Toxicology, 1979.
[47] D. Meyer, M. Marin-Kuan, E. Debon, P. Serrant, C. Bezançon, B. Schilte, G.E. Morlock, Breakthrough Genotoxicity Assay: New validated HPTLC-SOS-Umu-C assay *versus* state-of-the-art assays, in submission
[48] V. Glavnik, I. Vovk, A. Albreht, High performance thin-layer chromatography–mass spectrometry of Japanese knotweed flavan-3-ols and proanthocyanidins on silica gel plates, J. Chromatogr. A. (2017) 1482, doi:10.1016/j.chroma.2016.12.059.
[49] H. Strosse, H. Schoofs, B. Panis, E. Andre, K. Reyniers, R. Swennen, Development of embryogenic cell suspensions from shoot meristematic tissue in bananas and plantains (Musa spp.), Plant Sci. 170 (2006) 104–112.
[50] H. Strosse, E. Andre, L. Sági, R. Swennen, B. Panis, Adventitious shoot formation is not inherent to micropropagation of banana as it is in maize, Plant Cell. Tissue Organ Cult. 95 (2008) 321.
[51] A.M. Makara, P.R. Rubaihayo, M.J.S. Magambo, Carry-over effect of Thidiazuron on banana *in vitro* proliferation at different culture cycles and light incubation conditions, Afr. J. Biotechnol. 9 (2010) 3079–3085.
[52] G.R. Rout, S.K. Senapati, S. Aparajita, S.K. Palai, Studies on genetic identification and genetic fidelity of cultivated banana using ISSR markers, Plant Omics 2 (2009) 250.
[53] E.K. Sales, N.G. Butardo, Molecular analysis of somaclonal variation in tissue culture derived bananas using MSAP and SSR markers, Int. J. Biol. Vet. Agric. Food Eng. 8 (2014) 63–610.
[54] T. Mishra, A.K. Goyal, A. Sen, Somatic embryogenesis and genetic fidelity study of the micropropagated medicinal species, Canna indica, Horticulturae. 1 (2015) 3–13.
[55] I.Y. Rabbi, P.A. Kulakow, J.A. Manu-Aduening, A.A. Dankyi, J.Y. Asibuo, E.Y. Parkes, T. Abdoulaye, G. Girma, M.A. Gedil, P. Ramu, Tracking crop varieties using genotyping-by-sequencing markers: a case study using cassava (Manihot esculenta Crantz), BMC Genet. 16 (2015) 115.
[56] D. Ellis, O. Chavez, J.J. Coombs, J.V. S.oto, R. Gomez, D.S. Douches, A. Panta, R. Silvestre, N.L. Anglin, Genetic identity in genebanks: application of the SolCAP 12K SNP array in fingerprinting and diversity analysis in the global in trust potato collection, Genome. 61 (7) (2018) 523–537.
[57] A. Brito, J.E. Ramirez, C. Areche, B. Sepúlveda, M.J. Simirgiotis, HPLC-UV-MS profiles of phenolic compounds and antioxidant activity of fruits from three citrus species consumed in Northern Chile, Molecules 19 (2014) 17400–17421, doi:10.3390/molecules191117400.
[58] T.S. Teixeira, R.C. Vale, R.R. Almeida, T.P.S. Ferreira, L.G.L. Guimarães, Antioxidant potential and its correlation with the contents of phenolic compounds and flavonoids of methanolic extracts from different medicinal plants, Rev. Virtual Química. 9 (2017) 1546–1559.
[59] ... G. Mandalari, R.N. Bennett, G. Bisignano, D. Trombetta, A. Saija, C.B. Faulds, A. Narbad, Antimicrobial activity of flavonoids extracted from bergamot (Citrus bergamia Risso) peel, a byproduct of the essential oil industry, J. Appl Microbiol. 103 (6) (2007) 2056–2064.
[60] A. Ghasemzadeh, V. Omidvar, H.Z.E. Jaafar, Polyphenolic content and their antioxidant activity in leaf extract of sweet potato (Ipomoea batatas), J. Med. Plants Res. 6 (2012) 2971–2976.
[61] C.A.C. Araujo, L.L. Leon, Biological activities of Curcuma longa L., Mem. Inst. Oswaldo Cruz. 96 (2001) 723–728.
[62] Z. Lu, Q. Jia, R. Wang, X. Wu, Y. Wu, C. Huang, Y. Li, Hypoglycemic activities of A-and B-type procyanidin oligomer-rich extracts from different Cinnamon barks, Phytomedicine 18 (2011) 298–302.
[63] H. Matsuda, Y. Pongpiriyadacha, T. Morikawa, M. Ochi, M. Yoshikawa, Gastroprotective effects of phenylpropanoids from the rhizomes of Alpinia galanga in rats: structural requirements and mode of action, Eur. J. Pharmacol. 471 (2003) 59–67.
[64] D. Mohapatra, S. Mishra, N. Sutar, Banana and its by-product utilisation: an overview, J. Sci. Ind. Res. 69 (2010) 323–329.
[65] S. Kumar Karan, S.K. Mishra, D. Pal, A. Mondal, Isolation of β-sitosterol and evaluation of antidiabetic activity of Aristolochia indica in alloxan-induced diabetic mice with a reference to in-vitro antioxidant activity, J. Med. Plants Res. 6 (2012) 1219–1223, doi:10.5897/JMPR11.973.
[66] J.A. Schneider, Z. Arvanitakis, S.E. Leurgans, D.A. Bennett, The neuropathology of probable Alzheimer disease and mild cognitive impairment, Ann. Neurol. Off. J. Am. Neurol. Assoc. Child Neurol. Soc. 66 (2009) 200–208.
[67] K. Hostettmann, A. Borloz, A. Urbain, A. Marston, Natural product inhibitors of acetylcholinesterase, Curr. Org. Chem. 10 (2006) 825–847.
[68] R. Rhabasa-Lhoret, J.L. Chiasson, Alpha-glucosidase inhibitors, in: R.A. Defronzo, E. Ferrannini, H. Keen, P. Zimmet (Eds.), International Textbook of Diabetes Mellitus, Vol. 1, John Wiley, UK, 2004.
[69] W. Abeysekera, A. Chandrasekera, P.K. Liyanage, Amylase and glucosidase enzyme inhibitory activity of ginger (Zingiber officinale Roscoe) an *in vitro* study, Trop. Agric. Res. 19 (2007) 128–135.
[70] E.G. Asuquo, C.E. Udobi, Antibacterial and toxicity studies of the ethanol extract of Musa paradisiaca leaf, Cogent. Biol. 2 (2016) 1219248.
[71] A. Umamaheswari, A. Puratchikody, S.L. Prabu, T. Jayapriya, Phytochemical screening and antimicrobial effects of Musa acuminata bract, Intl. Res. J.Pharm. 8 (2017) 41–44, doi:10.7897/2230-8407.088142.
[72] J. Abirami, P. Brindha, C.D. Raj, Evaluation of toxicity profiles of Musa paradisiaca L (Pseudostem) Juice, Int. J. Pharm. Pharm. Sci. 6 (2014) 9–11.
[73] E.A. Ugbogu, V.C. Ude, I. Elekwa, U.O. Arunsi, C. Uche-Ikonne, C. Nwakanma, Toxicological profile of the aqueous-fermented extract of Musa paradisiaca in rats., Avicenna J. Phytomedicine. 8 (2018) 478–487.
[74] N. Barua, M. Das, An overview on the pharmacological activity of Musa sapientum and Musa paradisiaca, Intl. J. Pharma Prof. Res. 4 (2013) 986–992.
[75] P. Khawas, S.C. Deka, Comparative nutritional, functional, morphological, and diffractogram study on culinary banana (Musa ABB) Peel at various stages of development, Int. J. Food Prop. 19 (2016) 2832–2853, doi:10.1080/10942912.2016.1141296.
[76] S. López, J. Bastida, F. Viladomat, C. Codina, Acetylcholinesterase inhibitory activity of some Amaryllidaceae alkaloids and Narcissus extracts, Life Sci. 71 (2002) 2521–2529.
[77] P.K. Mukherjee, V. Kumar, M. Mal, P.J. Houghton, Acetylcholinesterase inhibitors from plants, Phytomed 14 (2007) 289–300.
[78] C. Vilela, S.A. Santos, J.J. Villaverde, L. Oliveira, A. Nunes, N. Cordeiro, C.S.R. Freire, A.J. Silvestre, Lipophilic phytochemicals from banana fruits of several *Musa* species, Food Chem. 162 (2014) 247–252.
[79] E. Mahran, I. Elgamal, M. Keusgen, G. Morlock, Effect-directed analysis by high performance thin-layer chromatography for bioactive metabolites tracking in *Primula veris* flower and *Primula boveana* leaf extracts, J. Chromatogr. A 1605 (2019) in print.